19th Symposium IMEKO TC 4 Symposium and 17th IWADC Workshop
Advances in Instrumentation and Sensors Interoperability
July 18-19, 2013, Barcelona, Spain

Quasi-analytical Design of a Square Helmholtz Coil with Finite Cross-sectional Area as a Magnetic Flux Density Standard

Sakda Somkun[1], Thepbodin Borirak-Arawin[2]

[1]*Now at School of Renewable Energy Technology, Naresuan University*
Phitsanulok, 65000, Thailand, e-mail: sakdaso@nu.ac.th
[2]*Magnetics Laboratory, National Institute of Metrology, Thailand (NIMT)*
3/4-5 Moo 3, Klong 5, Klong Luang, Pathumthani, 12120, Thailand, e-mail: thepbodin@nimt.or.th

Abstract- This paper describes a design methodology of a square Helmholtz coil with finite cross-sectional area to be used as a magnetic flux density standard up to 50 mT at NIMT. Magnetic field inside the square Helmholtz coil was considered to be assembled from the magnetic fields produced by every pair of square loops, which were analytically derived from the Biot-Savart law. This design technique, based on physical properties of the copper wires, allows the coil resistance to be easily predicted to match the output characteristics of the DC power supply. Temperature rise in the coil and the decrease of the coil constant due to thermal expansion were also taken into account. The calculated magnetic field was found to be closely agreed with finite element modelling (FEM). A design prototype was constructed and results showed good agreements with the numerical calculation.

I. Introduction

Helmholtz coils are widely used as magnetic field sources in calibration systems of magnetic field measuring instruments [1], [2]. Square Helmholtz coils provide better field homogeneity over the common circular configuration with a trade-off in the maximum field intensity [3]. In general, design of Helmholtz coils is based on calculation of the axial field derived from the Biot-Savart law, where the conductor is approximated to be infinitesimal [3]. In order to achieve a higher flux density, a number of turns have to be used causing the cross section to be thick compared to the coil width. Franzen [4] proposed a calculation method for Helmholtz coils with finite cross section, where choices of width to height ratios of the conductor cross section can be chosen. However, Franzen's method is applicable for the circular Helmholtz coils only. Kuns [5] presented an analytical method for calculation of magnetic field inside a plasma chamber by summing magnetic fields produced by individual conductor loops.

Thus, this paper describes a design method for of a square Helmholtz coil based on analytical calculation of every pair of square conductor loops, with a maximum centre flux density of 50 mT. Limited power constraints of the DC current source, temperature rise and thermal expansion in the coils were also taken into account.

II. Design methodology

A. Calculation of magnetic field

Figure 1(a) illustrates the square Helmholtz coil configuration, consisting of a pair of *N* turn square wire loops. Each has the width of $2a$ and they are separated by a distance of $2c$. The conductor diameter is considered to be infinitesimal. Its magnetic field along the *z* direction, B_z is of interest, which is derived from the well known Biot-Savart law given as

$$B_z = \frac{\mu_0 IN}{4\pi}\sum_{i=1}^{2}\sum_{j=1}^{2}(-1)^{i+j}\sum_{k=1}^{2}\left(\frac{(x-x_i)(y-y_j)}{\sqrt{(x-x_i)^2+(y-y_j)^2+(z-z_k)^2}}\left[\frac{1}{(x-x_i)^2+(z-z_k)^2}+\frac{1}{(y-y_j)^2+(z-z_k)^2}\right]\right) \quad (1)$$

where μ_0 is the permeability of free space, and $x_1 = y_1 = a$, $x_2 = y_2 = -a$, $z_1 = c$, $z_2 = -c$. The value of coil space of $c = 0.544506a$ was reported to be satisfied the Helmholtz condition [3]. In order to increase the flux density at the coil centre, higher current and turn numbers must be used. However, the insulation and thermal expansion of the copper wire limits the maximum coil current. On the other hand, increasing the turn numbers creates the conductor cross section not to be negligible compared to the coil width. This makes the axial flux density deviates from the Helmholtz condition in (1). In this case, the finite conductor cross section into account has to be taken into consideration. Figure 1(b) shows the cross section of a square Helmholtz coil. Each coil comprises *M* layers of round conductors with diameter of *d*. Each layer has *N* turns for the odd layers and *N*-1 for the even layers. This coil configuration can be considered to be assembled from individual pairs of single turn square loops located at turn *n* and layer *m*. The axial magnetic flux density produced by each pair of square loop, $B_{z_{nm}}$ can be easily calculated using (1). Their individual coil width, a_m and coil space c_n are defined as follows

$$a_m = a - H/2 + d/2 + (m-1)\frac{\sqrt{3}}{2}d \quad (2)$$

$c_n = c - W/2 + d \times (n - 1/2)$ for *m*=odd numbers; $c_n = c - W/2 + d \times n$ for *m*=even numbers (3)

, where a and c are the average coil width and coil space respectively, and W and H are the width and height of the conductor cross section. The total axial magnetic flux density, B_z is then the summation of each loop pair $B_{z_{nm}}$ given by

$$B_z = \sum_{m=1}^{M}\sum_{n=1}^{N} B_{zmn} \cdot \quad (4)$$

Equations (1)-(4) can be easily implemented in a spread sheet program or in MATLAB m-file, which is more economical and requires less computing power than a finite element package.

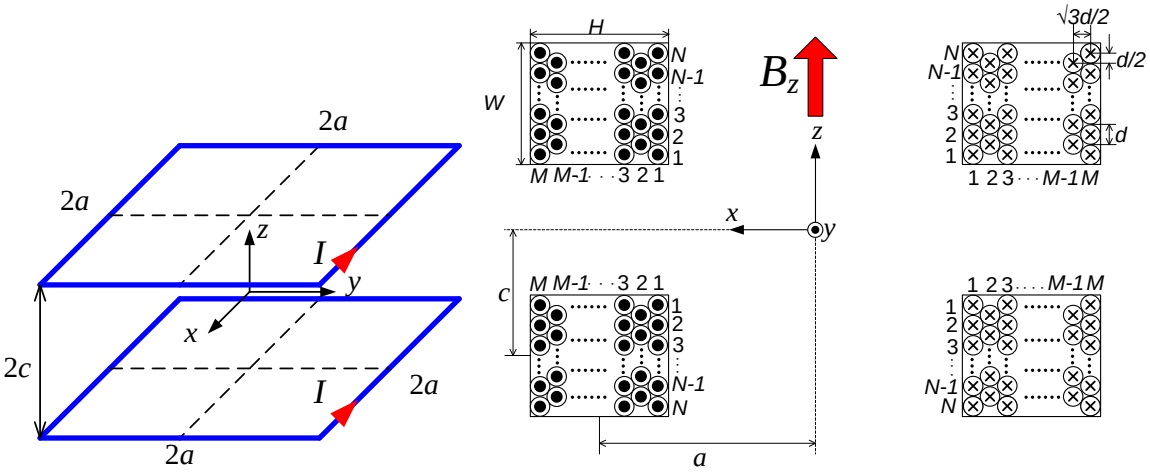

(a) (b)

Figure 1. (a) Filamentary square Helmholtz coil, (b) Cross section of a thick square Helmholtz coil

B. Design under power constraints

The maximum rating of a DC power supply at NIMT magnetics laboratory is 30 A at 70 V [6]. Thus, the size of copper wires had to be carefully selected to keep coil voltage and current at the maximum flux density below the power supply rating. Coil resistance R was determined from the coil geometry from

$$R = \rho\frac{l}{A} \quad (4)$$

, where A is the cross sectional area, l is the length, and ρ is the resistivity of the copper wire respectively. According to the copper wire specification, ρ/A at 20°C is provided [7]. Thus, the coil resistance was calculated from only the coil length

$$l = l_1 + l_2 \quad (5)$$

, where l_1 and l_2 are defined as follows

$$l_1 = 16\sum_{m=1}^{M} a_m \times N \quad \text{for odd layers} \quad (6)$$

$$l_2 = 16\sum_{m=1}^{M} a_m \times (N-1) \quad \text{for even layers.} \quad (7)$$

C. Temperature rise prediction

Helmholtz coils are usually fed with a constant current, I and assume that there is no heat exchange, so the change in the coil temperature can be predicted the energy supplied to the coil ($I^2R \cdot \Delta t$)

$$C_m = \frac{1}{m} \cdot \frac{I^2 R \cdot \Delta t}{\Delta T} = \frac{1}{m} \cdot I^2 \cdot \left(\frac{\rho l}{A} \right) \cdot \frac{\Delta t}{\Delta T} \tag{8}$$

where C_m is the specific heat capacity of the copper windings (385 J/kg·C), Δt is the time change after applying the coil current, m is the mass the copper wire. The copper wire specification sheet also gives the value of l/m [7], resulting in the temperature change can be predicted from

$$\Delta T = \left(\frac{l}{m} \right) \cdot \left(\frac{\rho}{A} \right) \cdot \frac{I^2 \Delta t}{C_m}. \tag{9}$$

It can be observed that the increase in the coil temperature depends only on the physical properties of the copper wire.

D. Thermal expansion

Decrease of the coil constant, k_s ($k_s = B/I$) due to thermal expansion in the coil and former materials is normally found in standard Helmholtz coils [8]. It is assumed that the effect of thermal expansion causes the coil width, a to increase with ΔT as $a = a_0(1+\alpha\Delta T)$, where a_0 is the initial coil width and α = 17 × 10^{-6} °C^{-1} is the thermal expansion coefficient of copper [9]. In fact, the coil constant, k_s is proportional to $1/a$ [3]. Thus, the effect of self heating on the coil constant can be written as

$$\frac{k_s}{k_{s0}} = \frac{1}{(1+\alpha\Delta T)} \tag{10}$$

where k_{s0} is the initial coil constant. It should be noted that the thermal expansion of the former material is neglected.

D. Design procedure

Figure 2 details the design procedure of a thick square Helmholtz coil. It begins with the calculation of a filamentary coil, providing initial information (coil width, coil space, and turn number/current ratio) for the thick coil. If the resistance of the calculated thick coil does not match the output characteristic of the power supply, the wire size has to be changed.

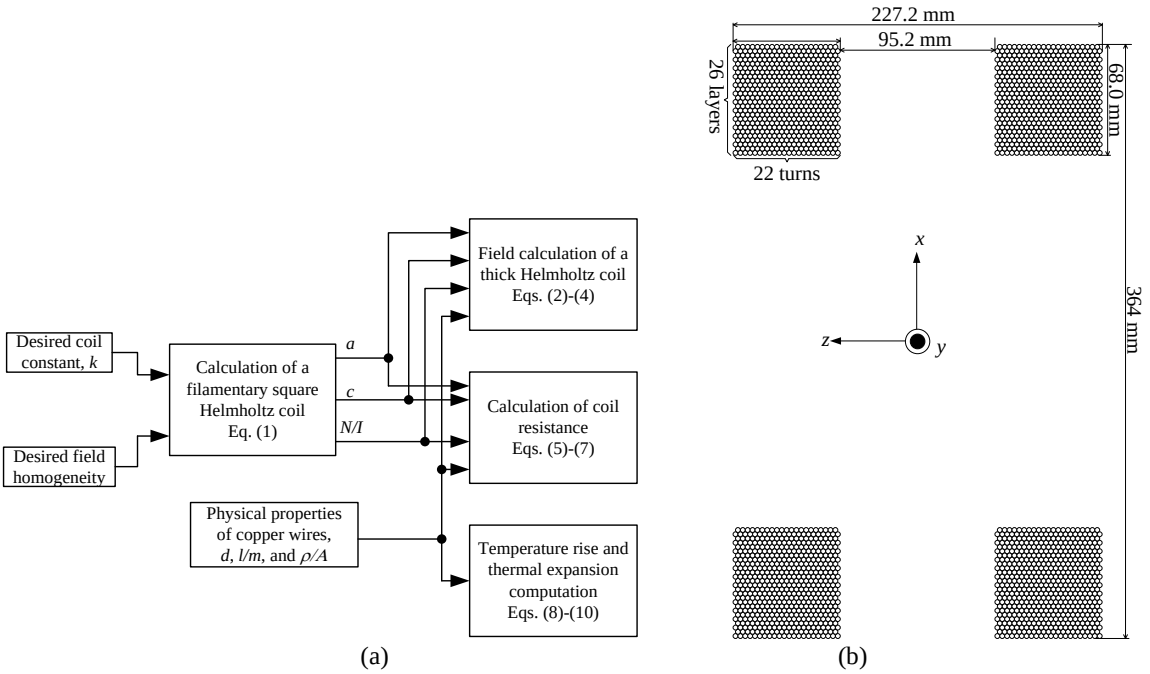

Figure 2. (a) Design procedure of a thick square Helmholtz coil, (b) Cross section geometry of the designed square Helmholtz coil

D. Numerical results

The criteria for the square Helmholtz coil in this design were to produce the maximum flux density of 50 mT with an excitation current less than 17 A, and field homogeneity along the axial direction (*z*) range of ±15 mm within 0.01 %. Table 1 compares two design choices met the requirement above. Coil#1 with the conductor diameter of 2.6 mm has the resistance of 5.4 and current at 50 mT of 13 A. This will easily the maximum rating of the power supply when coil resistance increases due to self heating. Thus, coil#2 with the wire diameter of 2.9 mm was then chosen for implementation. Figure 2(b) depicts the cross section geometry of the coil#2 which has 559 turns each coil. Flux density of this coil configuration was also calculated using 3D finite element modelling (FEM) to verify the proposed design scheme. Figure 3(a) shows that B_z of the designed thick coil along the *z* direction agrees with the filamentary coil with similar coil width and coil space. The FEM calculation of B_z also confirms this proposed method. The distribution of B_z to the flux density at the centre B_{z0} in the *xz* plane in Figure 3(b) also exhibits the typical characteristic of Helmholtz coils, where the field distribution is flat around the centre region.

Table 1. Comparison of two design choices of square Helmholtz coils

Coil	Coil geometry [mm]				Wire parameters			I @ 50mT [A]	R [Ω]	V_c [V]	ΔT @ 5min [°C]	Δk_s [%]
	a	c	W	H	d [mm]	ρ/A [Ω/km]	m/l [kg/km]					
1	145	79.0	69.5	70.1	2.6	3.324	47.77	13.00	5.4	70	9.16	-0.0156
2	150	82.0	70.8	67.1	2.9	2.665	59.36	16.34	3.5	57	9.34	-0.0159

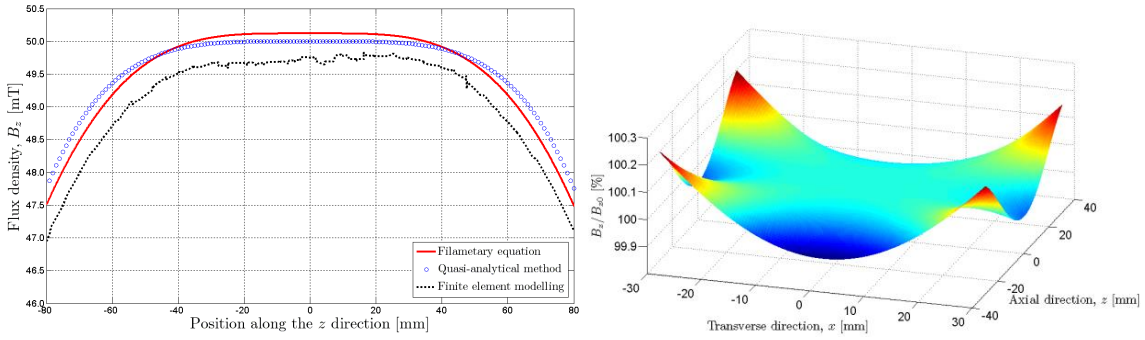

(a) (b)

Figure 3. (a) B_z produced by a filamentary square Helmholtz coil compared with a thick coil calculated by the quasi-analytical method and FEM, (b) Image of a design prototype under construction

D. Construction and test of the prototype coil

Figure SWG11 copper wires coated by polyester-imide/polyamide-imide, which can withstand temperature up to 200°C, were used as the conductors. Their physical properties are listed in Table 1. The coil former and base were constructed from Bakelite thanks to its resistivity to electricity and heat. They are assembled together with polyether ether ketone (PEEK) screws because of their robustness. Figure 4(b) exhibits the experiment setup for measurement of the coil constant of the prototype. The Helmholtz coil was fed by a constant current and its flux density was measured by a continuous wave NMR magnetometer from Echo Electronics model EFM-2000AX in the form of resonance frequency of the proton rich NMR sample. An Agilent 53131A universal counter locked by a 10 MHz standard frequency from a Cesium clock was used to measure the resonance frequency, f_r, which was then convert to flux density by

$$B_z = \frac{2\pi f_r}{\gamma'_p} \tag{11}$$

where γ'_p =2.675 153 268 × 10^8 s^{-1} T^{-1} is the shielded proton gyromagnetic ratio [10]. The temperature rise in the prototype coil was monitored by the coil voltage and a type J thermocouple attached on the wiring. The coil constant was observed in this experiment instead of the flux density to minimise the effect from fluctuation of the excitation current. The coil was positioned along the East-West direction. Test of the decrease of the coil constant due to temperature change was conducted around 50 mT. Determination of the field distribution was done approximately at 40 mT and the coil temperature was controlled not to exceed 28°C in order to limit

ISBN-10: 84-616-5438-2 | ISBN-13: 978-84-616-5438-3

measurement uncertainties due to the self heating effect. Each measurement point was carried out under positive and negative current polarities and the average taken to minimise the presence of the Earth magnetic field. Each was repeated five times. The laboratory temperature and humidity were controlled within 23°C ± 2 °C and 50 % ± 10 %.

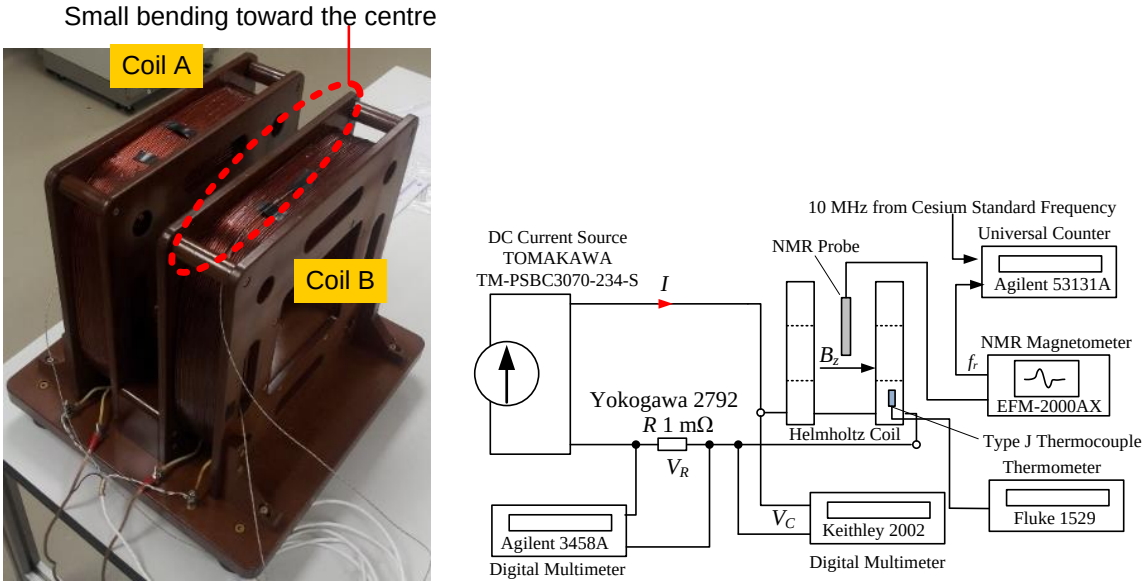

(a) (b)

Figure 4. (a) Photograph of the square Helmholtz coil, (b) Measurement setup

III. Experimental results and discussion

It was found that achieving a centre flux density of 50 mT required a current of 16.64 A. This means the prototype Helmholtz coil has the experimental coil constant of 3.005 mT/A ± 0.04 %, which is approximately 98.2 % of the calculated value (50/16.34 = 3.06 mT/A). The coil resistance was measured by a Keithley 2002 digital multimeter and found to be approximately 3.2 Ω at 22°C. The experimental coil constant and resistance lower than the calculation are believed to be due to the copper wire were not placed precisely as shown in Figure 2(b) resulting in lower total turns.

Figure 5 displays the increase in the coil temperature and the coil constant drops as a function of the coil temperature after feeding a constant current of 16.64 A. Both two variables show good agreements with (9) and (10). However, the measured temperature increased at a slower rate than predicted. This can be due to there was heat exchange with the surrounding environment and the prototype coil is not a lump element of copper as assumed in (9). The coil constant was estimated to drop about 0.016 % with a temperature rise of 10°C as given in Table 1, but the experimental result show that the winding can go up to around 13°C to cause the same order of reduction. This could be the copper wires were tighten on the former creating interacting forces that caused the wires not to elongate freely as predicted in (10).

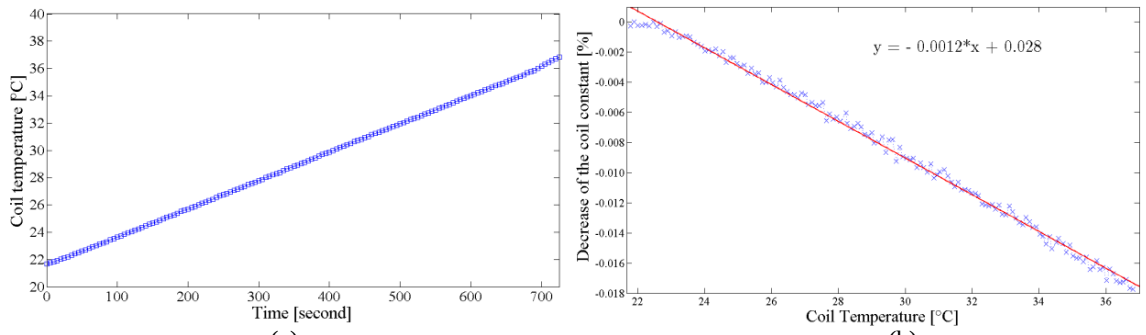

(a) (b)

Figure 5. (a) Temperature rise in the Helmholtz coil windings supplied by a constant current of 16.64 A, (b) Decrease of the coil constant against the coil temperature.

ISBN-10: 84-616-5438-2 | ISBN-13: 978-84-616-5438-3

Figure (6) compares the measured and calculated uniformities of magnetic field along the axial, *z* and transverse, *x* directions. It is noted that the uniformity was measured in the form of the coil constant because of the difficulty in keeping the current equal in every measurement. The deformation at the end plate of coil B shown on Figure 4(a) is believed to cause the unsymmetrical field distribution on the positive side of the *z* direction. In contrast, the measured field distribution on the negative side is close to the calculated value. The deformation also affects the uniformity on the *xy* plane, which can be seen in the field distribution along the *x* direction in Figure 6(b). Despite the imbalance of the field distributions, the centre region around 20 mm wide (-25 mm ≤ *z* ≤ 5 mm, and -20 mm ≤ *y* ≤ 10 mm) also has a good homogeneity better than ±0.05 %.

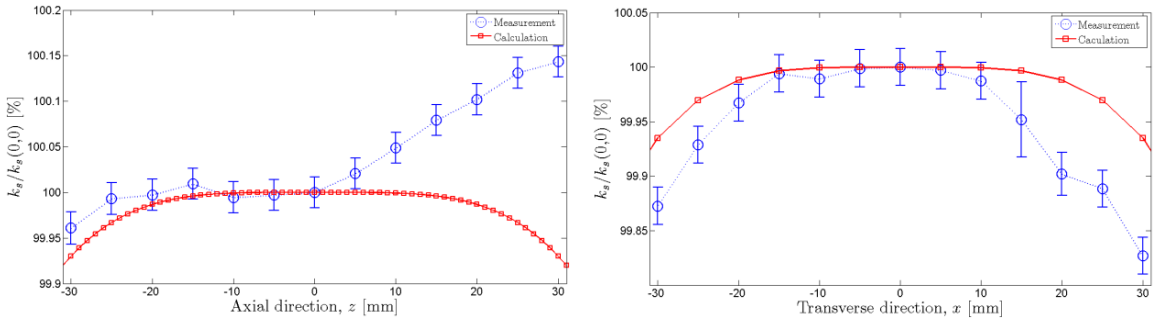

(a) (b)

Figure 6. Comparison of the measured and calculated uniformities of the coil constant: (a) along the axial, *z* direction, (b) along the transverse, *x* direction. The error bars represent the expanded uncertainties in the measurement (*k*=2).

IV. Conclusions

A square Helmholtz coil with finite cross section was designed to be used as a magnetic field source for calibration of flux density using the proposed quasi-analytical method based on Biot-Savart law, which required less computing power compared to FEM simulation. Physical propperties of coil conductors were directly fed into the design equations. This allowed the coil resistance to be accurately predicted to suite with the power supply output characteristics. Furthermore, temperture rise and reduction in the coil constant due to thermal expasion were also estimated. Finite lement modelling and practical implementation verified the effectiveness of the proposed design procedure. Construction Helmholtz coil coils should be done with great care in order to obtain the desired field distribution.

Acknowledgement

Authors are very grateful to National Science and Technology Development Agency (NSTDA), Thialand for the financial support of this project (research grant number SCH-NR2011-351).

References

[1] P. G. Park, Y. G. Kim, W. S. Kim, V. N. Kalabin, and V. Ya. Shifrin, "Precision calibration set-up for AC magnetic flux density measurement in the range of 1 Hz to 20 kHz*," Proceedings of the XIX IMEKO World Congress Fundamental and Applied Metrology*, Lisbon, Portugal, September 2009.

[2] M. Ishii, R. Ketzler, M. Albrecht, S. Kurokawa, Y. Shimada, "Improvement of formula and uncertaintyof the reference magnetic field for AC magnetometer calibration," accepted for publication in *IEEE Transactions on Instrumentation and Measurement*.

[3] W. M. Frix, G. G. Karady, and B. A. Venetz, "Comparison of calibration systems for magnetic measurement equipment," *IEEE Transactions on Power Delivery*, vol. 9, pp. 100-106, 1994.

[4] W. Franzen, "Generation of uniform magnetic fields by means of air-core coils," The Review of Scientific Instrumemts, vol. 33, pp. 933-938, 1962.

[5] K. Kuns, "Calculation of magnetic field inside plasma chamber," UCLA Technical Reports, [Online] Available: http://plasmalab.pbworks.com/f/bfield.pdf, 2007.

[6] Tomakawa TM-PSBC3070-234-S DC power supply user manual (in Japanese).

[7] Thai Hitachi Enamel Wire Co.,Ltd., http://www.theco.co.th/product-swg.php

[8] K. Weyand, "Compensation of the temperature coefficient of magnetic field coils," *IEEE Transactions on Instrumentation and Measurement*, vol. 54, pp. 713-717, 2005.

[9] D. C. Jiles, *Introduction to the principles of materials evaluation*, Boca Raton: CRC Press, 2008.

[10] P. J. Mohr, B. N. Taylor, and D. B. Newell, "CODATA recommended values of the fundamental physical constants: 2010," arXiv:1203.5425v1, pp. 1-94, 2012.